Scientific Research Publishing

International Journal of Geosciences, 2025, 16(11), 871-889
https://www.scirp.org/journal/ijg
ISSN Online: 2156-8367
ISSN Print: 2156-8359

Petrogenesis and Geodynamic Setting of Paleoproterozoic Rocks from Zoukougbeu (Dalao, Central-Western Côte d'Ivoire): Insights from Petrography and Geochemistry

Koffi Alexis N'dri[1*], Ziandjêdé Hervé Siagné[1], Brice Roland Kouassi[2], Ibrahima Aminata Diaby[3], Marc Éphrem Allialy[3], Yaya Ouattara[3], Gnanzou Allou[3]

[1]Laboratoire des Sciences Géographiques, du Génie Civil et des Géosciences, Ecole Supérieure des Mines et Géologie, Institut National Polytechnique Félix Houphouët-Boigny, Yamoussoukro, Côte d'Ivoire
[2]UFR Sciences Biologiques, Département Géosciences, Université Peleforo Gon-Coulibaly, Korhogo, Côte d'Ivoire
[3]Laboratoire de Géologie, Ressources Minérales et Énergétiques/Unité de Formation des Sciences de la Terre et des Ressources Minières, Université Félix Houphouët-Boigny, Abidjan, Côte d'Ivoire
Email: *ndri.alexis@yahoo.fr

How to cite this paper: N'dri, K.A., Siagné, Z.H., Kouassi, B.R., Diaby, I.A., Allialy, M.E., Ouattara, Y. and Allou, G. (2025) Petrogenesis and Geodynamic Setting of Paleoproterozoic Rocks from Zoukougbeu (Dalao, Central-Western Côte d'Ivoire): Insights from Petrography and Geochemistry. *International Journal of Geosciences*, **16**, 871-889.
https://doi.org/10.4236/ijg.2025.1611043

Received: October 15, 2025
Accepted: November 23, 2025
Published: November 26, 2025

Abstract

The Paleoproterozoic basement of Zoukougbeu in central-western Côte d'Ivoire lies within the southern Baoulé-Mossi domain of the West African Craton, a key area for understanding the crustal evolution associated with the Eburnean orogeny. However, the petrogenesis and geodynamic context of the granitoid intrusions in this region remain poorly constrained, despite their potential significance for regional crustal growth and mineralization. This study integrates petrographic and whole-rock geochemical data from drill-core samples to clarify the origin and tectonic evolution of these rocks. The lithological assemblage includes granodiorite, granite, diorite, gneiss, and pegmatite, variably deformed and hydrothermally altered. Petrographic analysis reveals plagioclase-quartz-biotite-amphibole assemblages overprinted by chlorite-epidote alteration, indicating greenschist- to amphibolite-facies metamorphism. Geochemically, the rocks define a calc-alkaline, metaluminous to slightly peraluminous suite with tonalite-trondhjemite-granodiorite (TTG) affinity. Their enrichment in large-ion lithophile elements and depletion in Nb-Ta-Ti, coupled with LREE enrichment and negative Eu anomalies, are typical of subduction-related magmatism. These signatures indicate that the Zoukougbeu granitoids originated from partial melting of hydrated basaltic crust with minor mantle input in a continental volcanic-arc setting during the Eburnean orogeny (~2.1 - 2.0 Ga). This finding refines the current understanding of Paleoproterozoic crustal evolution in the

southern West African Craton and highlights the role of arc magmatism in its stabilization.

Keywords

Petrogenesis, Geodynamic Setting, Petrography, Geochemistry, Côte d'Ivoire

1. Introduction

The West African Craton (WAC) represents one of the oldest and most stable continental blocks on Earth, comprising Archean and Paleoproterozoic terranes that amalgamated during successive orogenic cycles [1] [2]. Its southern segment, the Man-Leo Shield, preserves a well-exposed record of crustal evolution associated with the Eburnean orogeny (2.2 - 2.0 Ga), a pivotal event responsible for large-scale crustal growth, granitization, and gold mineralization across the Birimian domain [3]-[5]. Within Côte d'Ivoire, the Baoulé-Mossi domain contains extensive Paleoproterozoic granitoid complexes intruding metavolcanic and metasedimentary belts, which provide critical insights into the tectonic setting and magmatic processes that accompanied early Proterozoic crustal differentiation. The Zoukougbeu area, located in the Soubré Belt, Daloa region, central-western Côte d'Ivoire, occupies a transitional zone between Archean and Paleoproterozoic crustal domains. Despite its strategic position within the southern Birimian terranes, the petrogenetic and geodynamic evolution of its granitoids remains poorly constrained. Previous regional work has recognized TTG-type and calc-alkaline granitoids related to subduction-driven magmatism [6]-[8], yet detailed petrographic and geochemical studies of the Zoukougbeu intrusions are lacking.

This study aims to 1) characterize the mineralogical and geochemical features of the major lithological units, 2) determine the magmatic affinity and processes governing their evolution, and 3) infer the tectonic environment of their emplacement. By integrating petrographic observations with major, trace, and rare earth element geochemistry, this work contributes to refining the Paleoproterozoic crustal evolution model of the southern West African Craton and constrains the geodynamic framework associated with the Eburnean orogenic cycle.

2. Geological Setting

The study area lies within the southern part of the West African Craton (WAC), a large and stable continental block comprising Archean to Paleoproterozoic terranes that stabilized around 1.9 Ga [1] [2] (**Figure 1**). The WAC experienced two major orogenic cycles: the Liberian (3.0 - 2.5 Ga) and the Eburnean (2.5 - 1.8 Ga), which shaped its crustal architecture through granitization, metamorphism, and deformation. Structurally, the craton includes the Reguibat Rise in the north and the Man-Leo Shield in the south, separated by Paleoproterozoic volcanic-sedimentary belts. The Man-Leo Shield, extending from Liberia to Ghana, is

divided into two crustal domains: the Archean Kénéma-Man domain to the west and the Paleoproterozoic Baoulé-Mossi domain to the east (**Figure 1(a)**). These are separated by the N-S-trending Sassandra Fault Zone, a major lithospheric boundary that has been repeatedly reactivated since the Paleoproterozoic. The Archean domain is dominated by high-grade gneisses, charnockites, and migmatites formed during the Leonian and Liberian orogenies, whereas the Baoulé-Mossi domain consists mainly of Birimian metavolcanic and metasedimentary sequences intruded by syn- to late-tectonic granitoids emplaced during the Eburnean event [4] [9] [10]. In Côte d'Ivoire, the Precambrian basement covers more than 97% of the territory, overlain locally by Cenozoic sediments along the coast [11] (**Figure 1(b)**). The study area, located in the northern part of the Soubré Belt, occupies a transitional position between the Archean and Paleoproterozoic domains. It is composed of magmatic, metamorphic, and volcano-sedimentary units, including biotite granites, granodiorites, leucogranites, migmatitic gneisses,

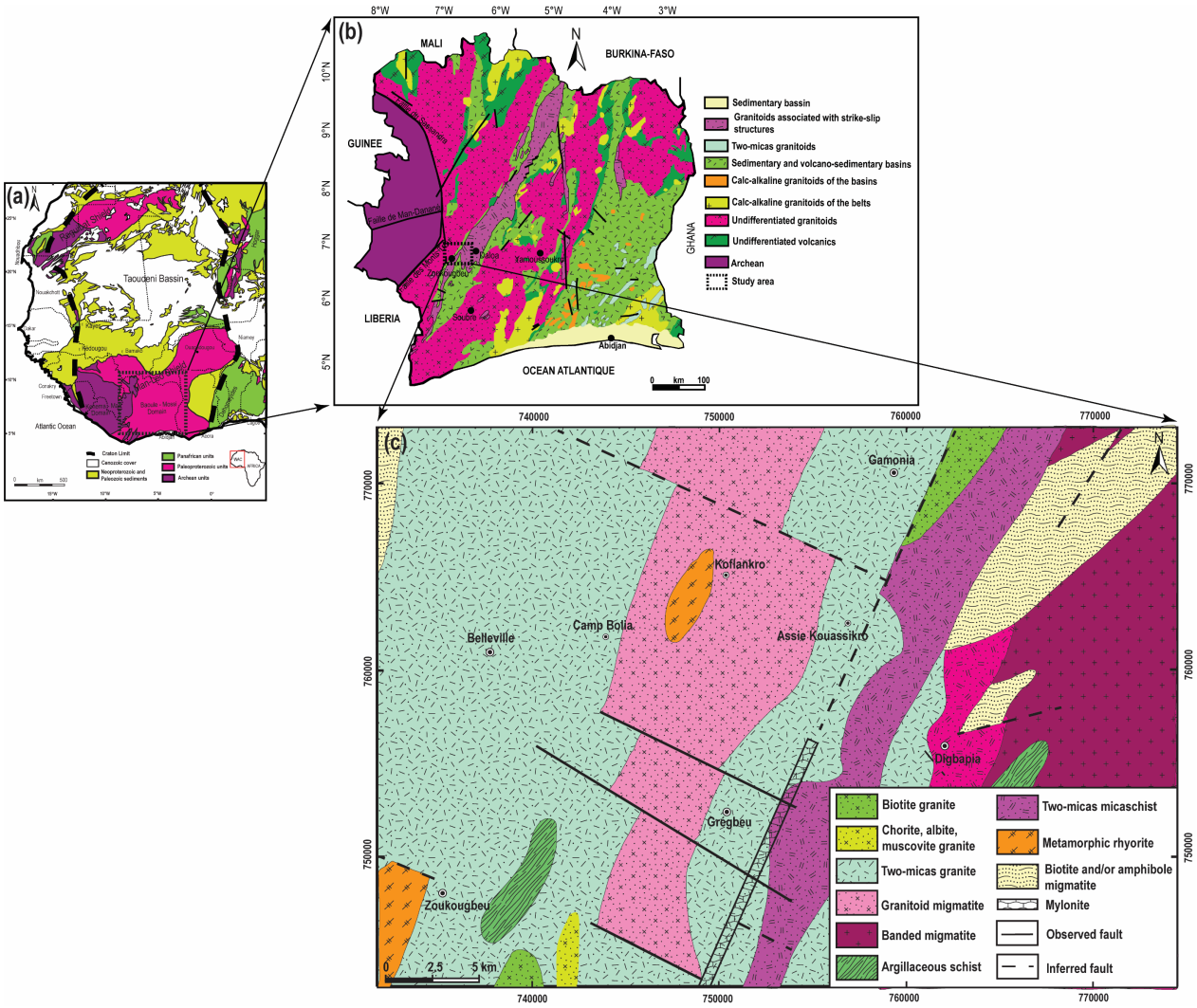

Figure 1. (a) Geological map of the West African Craton showing the location of the Ivory Coast (modified after [13]). (b) Simplified geological map of the Ivory Coast (modified after [14]). (c) Geological map of the Zoukougbeu area (modified after [15]).

schists, and amphibolites (**Figure 1(c)**). These rocks are locally cut by pegmatites, quartz veins, and doleritic dykes. Structurally, the region records multiple deformation and magmatic episodes related to the Liberian and Eburnean orogenies [12]. The earlier ductile events produced folding and granitization, while subsequent Eburnean deformation reactivated pre-existing structures, forming shear zones that guided later magmatic intrusions and hydrothermal systems. The reactivation of deep crustal faults such as the Sassandra Fault likely favored fluid circulation and gold mineralization, similar to other transcurrent shear zones within the Birimian terranes of the southern West African Craton.

3. Methodology

3.1. Sampling Strategy

Given the scarcity of surface outcrops in the region due to dense vegetation cover and extensive supergene alteration, sampling focused exclusively on diamond drill (DD) cores. A total of 14 representative rock samples were selected from various drill holes, covering the main lithological units identified in the Zoukougbeu area. The samples were carefully described, logged, and transported to the laboratory for subsequent analysis.

3.2. Petrographic Analysis

Petrographic characterization was conducted through integrated macroscopic and microscopic examination. Initial macroscopic analysis of diamond drill core samples focused on fundamental characteristics, including color, mineral assemblage, texture, and hydrothermal alteration features (silicification, chloritization, carbonatation). This preliminary assessment enabled lithological identification and selection of representative specimens for further investigation. Subsequently, fourteen (14) thin sections were prepared and examined using an Optika polarizing optical microscope equipped with a digital imaging system at the Laboratory of Geology, Mineral and Energy Resources (LGREM) of Félix Houphouët-Boigny University. Detailed microscopic observations under both plane-polarized and cross-polarized light enabled precise mineral identification, textural analysis, and documentation of metamorphic parageneses. This combined approach allowed comprehensive rock classification and characterization of alteration mineralogy across multiple scales of observation.

3.3. Geochemical Analysis

Eight representative rock samples, covering the main lithological varieties, were sent to Interteck Laboratory in Ghana for whole-rock geochemical analysis using Inductively Coupled Plasma Mass Spectrometry (ICP-MS). Sample preparation involved crushing and pulverizing to a fine powder. Approximately 15 - 20 mg of each powdered sample was used for analysis following standardized procedures. Various standards were used, and data quality assurance was verified by running these standards between samples as unknowns. The detection limits were 0.01

ppm for the REE and Y. Major elements (SiO_2, Al_2O_3, Fe_2O_3, MnO, MgO, CaO, Na_2O, K_2O, TiO_2, P_2O_5, Cr_2O_3) were quantified directly by ICP-MS. Volatile elements (As, Bi, Hg, Sb, Se, Te) underwent digestion by Aqua Regia prior to ICP-MS quantification. Trace elements (Ba, Be, Co, Cs, Ga, Hf, Nb, Rb, Sn, Sr, Ta, Th, U, V, W, Zr, Y, Nd, Cu, Pb, Zn, Ni, As, Cd, Sb, Bi) and Rare Earth Elements (La, Ce, Pr, Sm, Eu, Gd, Tb, Dy, Ho, Er, Tm, Yb, Lu) were subjected to lithium borate fusion followed by acid dissolution before ICP-MS analysis. The resulting geochemical data were used to construct classification and discrimination diagrams to determine the magmatic affinity, geochemical characteristics, and tectonic setting of the investigated rock suites.

4. Results

4.1. Petrography

The lithologies of the Zoukougbeu area were examined to characterize mineralogical composition, texture, and hydrothermal alteration relevant to gold mineralization. Thin-section analysis focused on granodiorite, gneiss, diorite, mylonitic granite, and pegmatite. Granodiorite is the dominant lithology and principal host of gold. It is medium-grained, mesocratic, and composed of plagioclase, quartz, K-feldspar, biotite, and amphibole. The rock is locally deformed, moderately altered, and commonly cut by quartz veins and veinlets. Microscopically, plagioclase is subhedral to euhedral, quartz is interstitial and anhedral, biotite is brownish-green and frequently contains zircon inclusions, and amphibole (green hornblende) is subhedral with partial alteration to epidote. Secondary chlorite and epidote are pervasive, and minor opaque minerals are present (**Figure 2(a)** and **Figure 2(b)**). Gneiss occurs as foliated metamorphic units with alternating light quartz-feldspar bands and darker ferromagnesian-rich layers composed of biotite and amphibole. Chloritization and epidotization are common. Quartz is abundant, anhedral to subrounded; plagioclase is subhedral to euhedral, occasionally containing quartz inclusions; biotite is subhedral, aligned along foliation planes, and locally hosts zircon; amphibole is subhedral to euhedral and occasionally fractured (**Figure 2(c)** and **Figure 2(d)**). Secondary chlorite and epidote impart green and yellow-orange hues. Diorite intrudes both gneiss and granodiorite and is dark, melanocratic, composed of plagioclase, amphibole, and biotite. It exhibits fine- to medium-grained hypidiomorphic textures. Plagioclase is anhedral and partially altered to epidote; biotite is euhedral to subhedral and partly transformed to chlorite; amphibole is subhedral with occasional quartz inclusions (**Figure 2(e)** and **Figure 2(f)**). Quartz is rare and interstitial. Secondary epidote and calcite are common, and minor opaque minerals are present. Mylonitic granite, observed in drill core ZOU06, is coarse-grained and leucocratic, comprising quartz, feldspar, muscovite, and biotite. Quartz forms large anhedral phenoblasts with undulose extinction. Plagioclase is subhedral to euhedral and locally deformed, biotite is subhedral to euhedral and preferentially oriented, and muscovite is medium-grained, subhedral, and associated with plagioclase (**Figure 2(g)** and **Figure 2(h)**). Pegma-

tites crosscut granodiorite, granite, and gneiss. They are coarse- to very coarse-grained, whitish to pinkish, and composed of quartz, K-feldspar, plagioclase, biotite, and muscovite. Overall, the petrography indicates a complex history of magmatic emplacement, deformation, and hydrothermal alteration. Granodiorite exhibits pervasive alteration of biotite and amphibole to chlorite and epidote, consistent with propylitic hydrothermal overprinting. Quartz veinlets and mylonitic textures indicate structurally controlled fluid migration along ductile-brittle shear zones. Gneiss and diorite represent competent basement lithologies locally overprinted by hydrothermal processes. Collectively, these features support a syn- to post-magmatic, deformation-assisted hydrothermal model for gold mineralization.

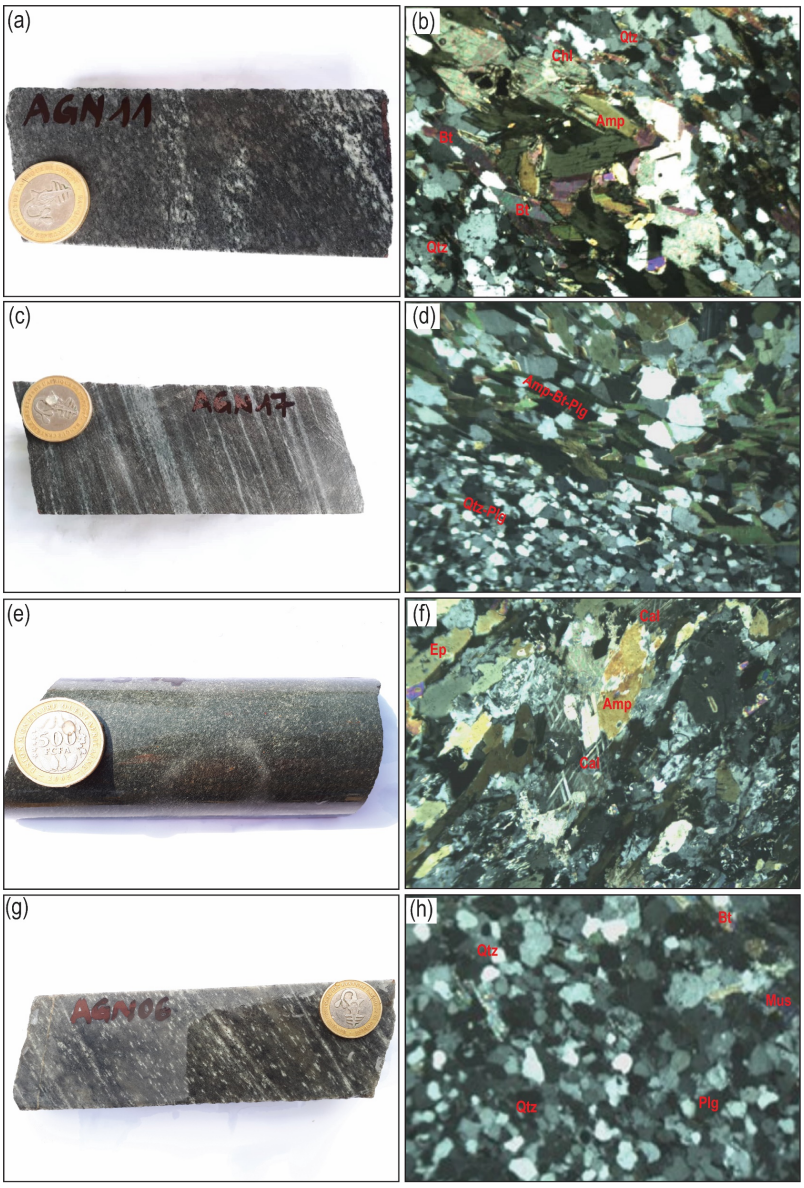

Figure 2. Macroscopic and microscopic aspects of the Zoukougbeu studied rocks. (a) - (b) Granodiorite, (c) - (d) Gneiss, (e) - (f) Diorite, and (g) - (h) Mylonite granite.

4.2. Geochemistry

4.2.1. Major Elements

1) Composition and Classification

Whole-rock geochemical data for eight representative samples from the Zoukougbeu area reveal a spectrum of felsic to intermediate compositions, delineating the principal lithological units. The sample ZOU06, representative of the granitic suite, is highly evolved, with a silica content of 75.0 wt.% and correspondingly low MgO (0.57 wt.%), Fe_2O_3 (2.14 wt.%), and TiO_2 (0.14 wt.%) (**Table S1** in Appendix Supplementary material). Its high-silica, low-mafic character is confirmed by its position in the granite field on the total alkalis-silica (TAS) diagram of [16] (**Figure 3(a)**). However, its sodic nature (Na_2O = 3.95 wt.%, K_2O = 1.91 wt.%) places it at the boundary between tonalite, trondhjemite, and granodiorite in the An-Ab-Or classification system of [17], suggesting a transitional trondhjemitic granite composition (**Figure 3(b)**). The granodioritic-tonalitic unit (samples ZOU11, ZOU15, ZOU23) exhibits lower silica contents (63.16 - 64.74 wt.%) and higher concentrations of mafic components (MgO = 2.29 - 2.98 wt.%; CaO = 4.55 - 5.51 wt.%) compared to the granite (**Table S1** in Appendix Supplementary material). The samples show a range in alkali contents, with Na_2O varying from 3.65 to 6.77 wt.%. On the TAS diagram, samples ZOU11 and ZOU23 plot definitively in the tonalite field, while ZOU15 falls near the tonalite-monzonite boundary (**Figure 3(a)**). This is refined by the An-Ab-Or diagram, which identifies ZOU15

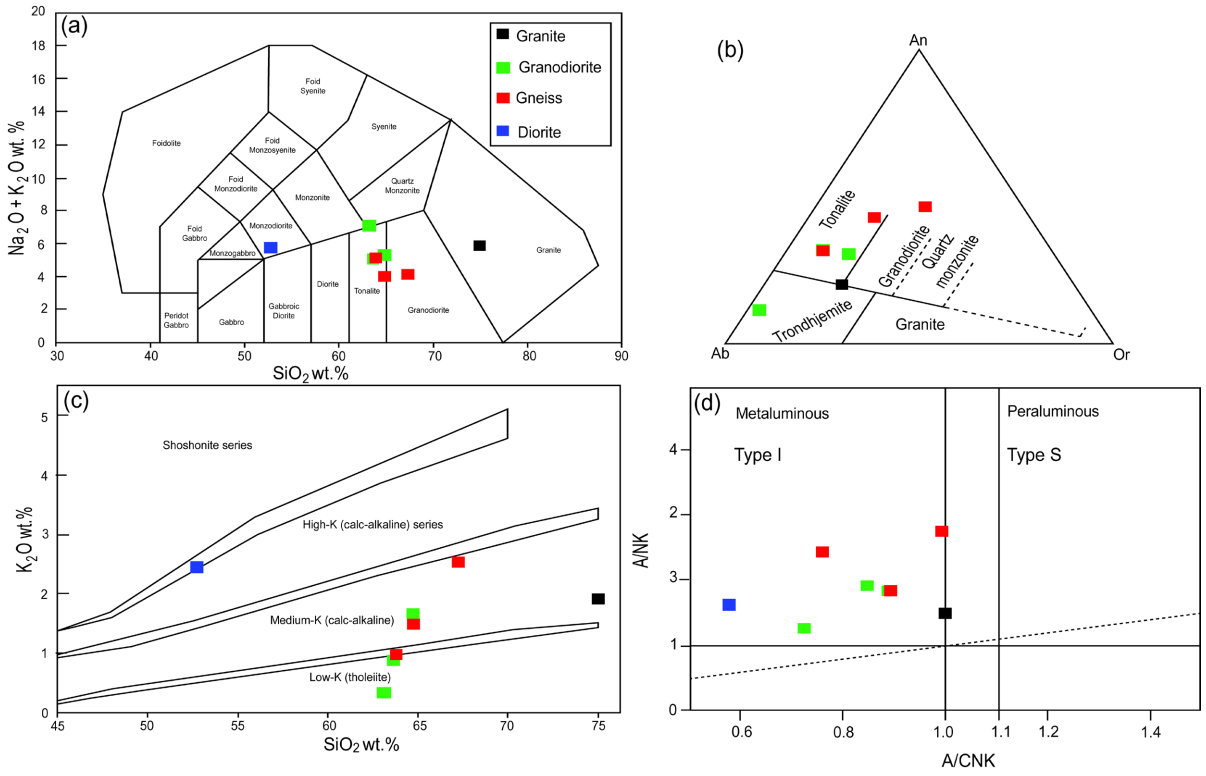

Figure 3. Chemical variation diagrams for the Zoukougbeu area rocks, illustrating the chemical features that distinguish each studied rock. (a) $Na_2O + K_2O$ vs. SiO_2 plot (after [16]), (b) Ternary An-Ab-Or plot (after [17]), (c) K_2O vs. SiO_2 plot (after [18]), and (d) A/NK vs. A/CNK plot (after [19]).

as having a trondhjemitic signature, highlighting the TTG (Tonalite-Trondhjemite-Granodiorite) affinity of this suite (**Figure 3(b)**). The gneissic samples (ZOU10, ZOU12, ZOU17) show moderately high silica contents (63.79 - 67.23 wt.%) (**Table S1** in Appendix Supplementary Material). Their compositions are variable, with ZOU10 and ZOU17 classified as tonalitic gneiss and ZOU12 as granodioritic gneiss based on both TAS and An-Ab-Or diagrams (**Figure 3(a)** and **Figure 3(b)**). This suggests their protoliths were part of the same TTG magmatic suite as the granodiorites. In contrast, sample ZOU16 is compositionally distinct, with a significantly lower SiO_2 content of 52.72 wt.% and a moderate total alkali content (Na_2O + K_2O = 5.76 wt.%). Its high K_2O (2.45 wt.%), CaO (7.92 wt.%) (**Table S1** in Appendix Supplementary Material), and compatible element contents are characteristic of a monzodiorite, representing a more mafic magmatic phase in the area.

2) Magmatic Series and Chemical Evolution

In the K_2O-SiO_2 diagram of [18], the Zoukougbeu rocks define a medium-K calc-alkaline series, whereas the diorite exhibits a high-K affinity (**Figure 3(c)**). This trend is characteristic of magmas formed in continental arc environments. In the A/NK-A/CNK diagram [19], the granodiorite, gneiss, and diorite show metaluminous compositions with A/CNK ratios of 0.72 - 0.89, 0.76 - 0.99, and 0.58, respectively, while the granite lies near the metaluminous-peraluminous boundary (A/CNK ≈ 1.0) (**Figure 3(d)**). These variations suggest increasing crustal involvement during magmatic differentiation. Harker diagrams (SiO_2 vs. major oxides) display linear and coherent trends (**Figure 4**), with negative correlations between SiO_2 and MnO, Al_2O_3, MgO, CaO, Na_2O, TiO_2, P_2O_5, and Fe_2O_3, and a strong positive correlation with K_2O. These relationships indicate fractional crystallization as the dominant process during magma evolution [20]. The decrease in Al_2O_3 with increasing SiO_2 reflects plagioclase fractionation, while K_2O enrichment marks late-stage crystallization of K-bearing minerals such as biotite and K-feldspar. Overall, the Zoukougbeu magmas evolved through calc-alkaline differentiation of a metaluminous to slightly peraluminous source under crustal magmatic conditions.

4.2.2. Trace Elements

Primitive mantle-normalized multi-element diagrams [21] reveal consistent patterns across the lithological suite (**Figure 5**). The sub-parallel nature of the spidergrams suggests a genetic relationship and a common magmatic source. All samples are characterized by significant enrichment in Large Ion Lithophile Elements (LILE; e.g., K, Pb) and pronounced negative anomalies in High Field Strength Elements (HFSE; notably Nb-Ta, Ti), alongside negative P anomalies. The granitic sample displays moderate to strong negative anomalies in Rb, Ba, Nb, Ta, and Ti. The granodiorites and gneisses show similar depletion patterns, with marked negative Nb-Ta anomalies, while the monzodiorite also exhibits a prominent Nb-Ta trough alongside lower Ce and Th abundances. Chondrite-normalized REE patterns [22] further elucidate magmatic history (**Figure 6**). The granite exhibits moderate Light Rare Earth Element (LREE) enrichment ((La/Yb)N = 12.29), a relatively flat Heavy REE (HREE) segment, and a distinct negative Eu anomaly (Eu/Eu* =

0.65), indicative of significant plagioclase fractionation (Table S1 in Appendix Supplementary material). The granodiorites and gneisses show similar, moderately fractionated REE patterns ((La/Yb) N = 13.48 - 19.48) with generally flat HREE profiles and variable negative Eu anomalies (Eu/Eu* = 0.74 - 0.97). In contrast, the monzodiorite is distinguished by a significantly higher total REE abundance (∑REE = 338.5 ppm), a strongly fractionated pattern ((La/Yb) N = 34.09), and the absence of an Eu anomaly, suggesting derivation from a different source or melting regime where plagioclase was not a residual phase. Collectively, the coherent trace element signatures—specifically the LILE enrichment coupled with Nb-Ta and Ti depletion—are classic geochemical fingerprints of magmatism in a subduction zone setting. The REE patterns and Eu systematics further constrain the role of fractional crystallization, particularly plagioclase separation, in the evolution of the felsic to intermediate rocks.

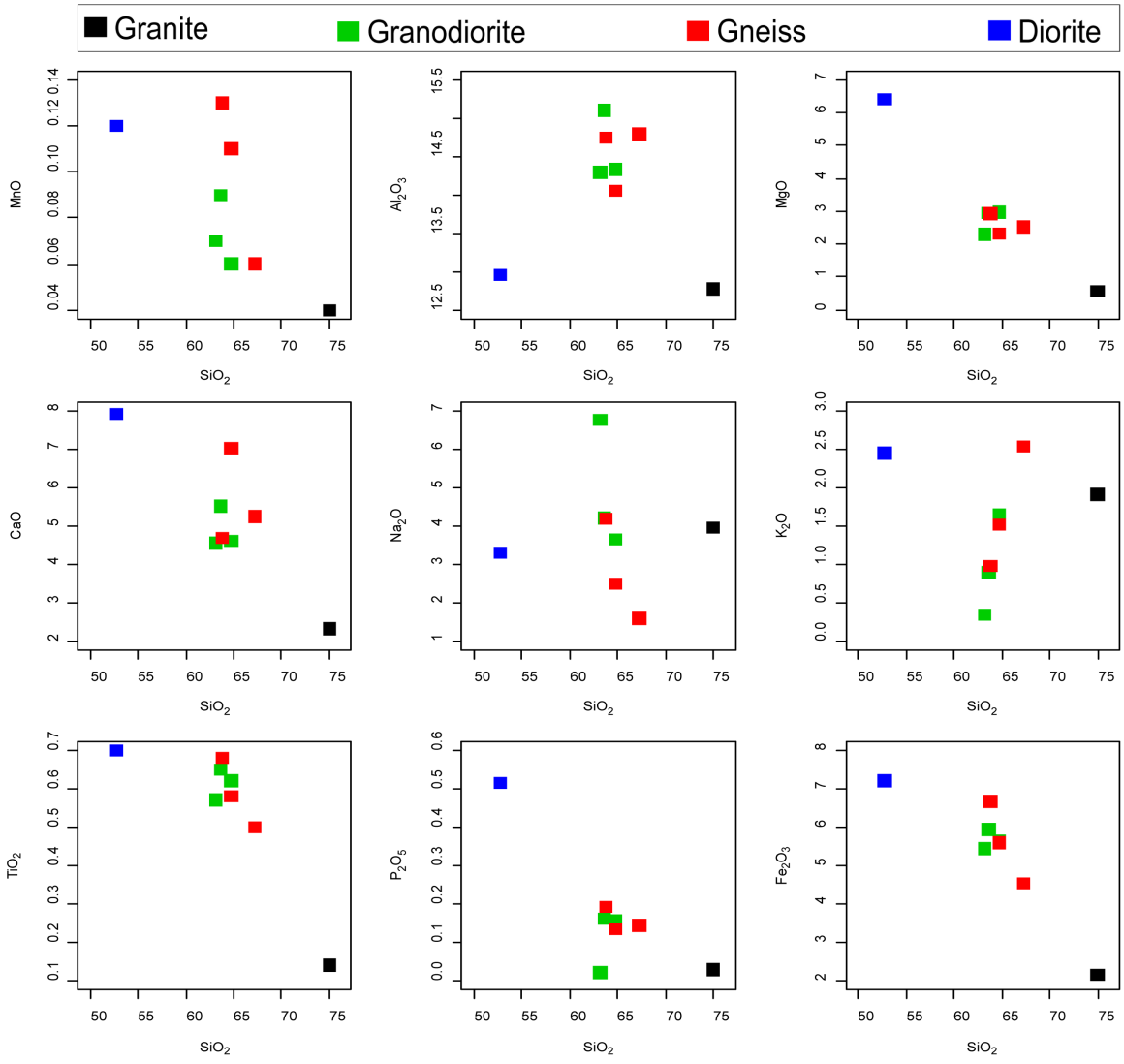

Figure 4. Harker diagrams of major elements for the rocks from the studied areas.

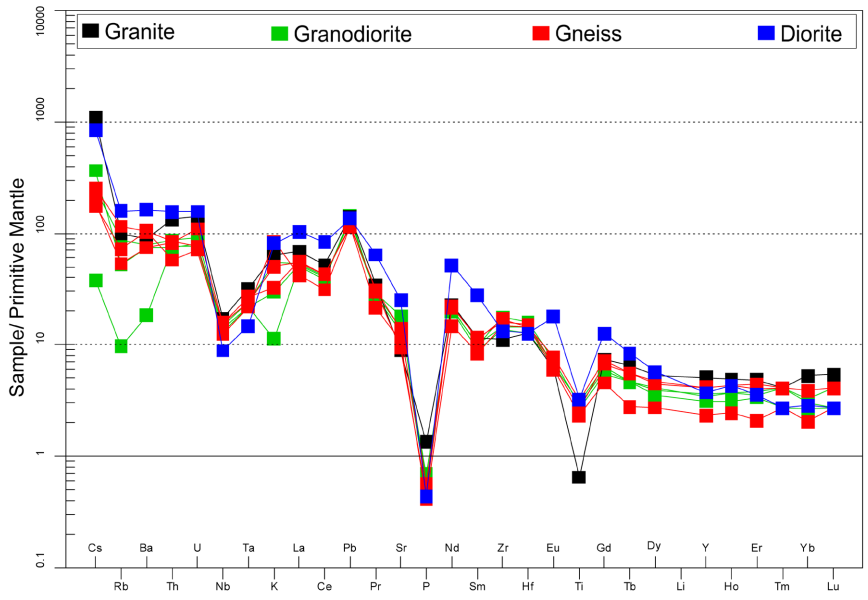

Figure 5. Primitive mantle-normalized multi-element spider diagrams for the Zoukougbeu studied rocks (Primitive mantle values from [21]).

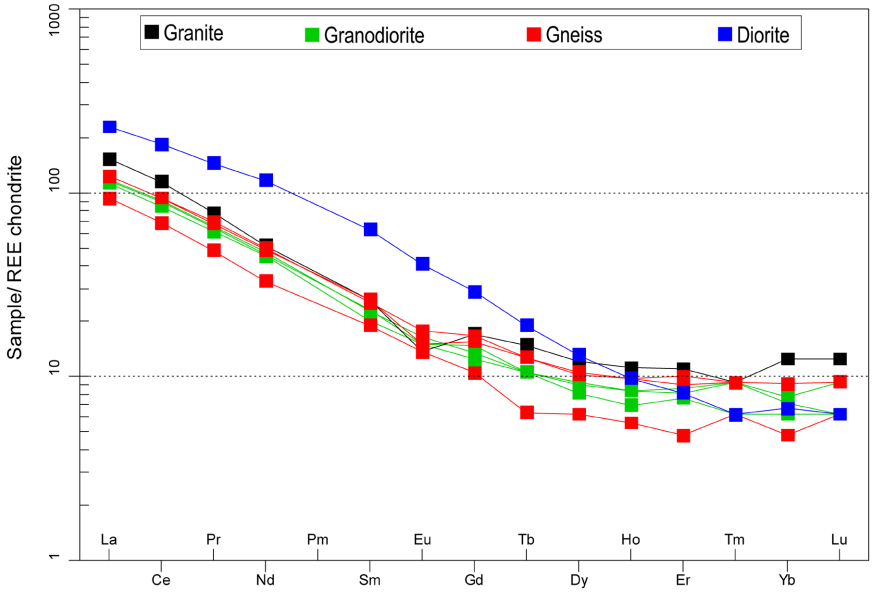

Figure 6. Chondrite-normalized rare earth element (REE) patterns for the Zoukougbeu studied rocks (Chondrite values from [22]).

5. Discussion

5.1. Petrographic Characteristics

Petrographic observations from the Zoukougbeu area in central-western Côte d'Ivoire reveal a lithological assemblage dominated by magmatic rocks—mylonitized granite, granodiorite, diorite, and pegmatite—together with gneissic units representing the metamorphic basement. These lithologies are consistent with

those previously described in the region [23]-[25], although the mylonitized granite identified here constitutes a new contribution to the lithostratigraphic framework. The granodiorite is the predominant lithology and constitutes the principal host of gold mineralization. It is mesocratic, locally hydrothermally altered, and composed mainly of quartz, plagioclase, biotite, and amphibole, with accessory pyrite and sphene. These mineralogical associations and hydrothermal features closely resemble those reported from other Birimian gold-bearing systems, such as Bonikro [26] and Daloa [15], suggesting a regional metallogenic control linked to hydrothermally altered granodioritic intrusions. The alteration assemblage—dominated by chlorite, epidote, and sericite—would reflect pervasive hydrothermal overprinting under greenschist-facies conditions, and locally would reach amphibolite facies. These metamorphic conditions are typical of the Paleoproterozoic Birimian terranes throughout West Africa [5] [27]-[31]. The abundance of low-pressure assemblages and the preservation of primary igneous textures suggest a low- to medium-grade regional metamorphism superimposed on pre-existing magmatic rocks, likely during the Eburnean orogeny.

5.2. Geochemical Constraints and Magmatic Affinity

Whole-rock geochemical data indicate that the granitoids of the Zoukougbeu area are calc-alkaline and metaluminous, plotting predominantly in the tonalite-trondhjemite-granodiorite (TTG) compositional field. This TTG signature is characteristic of many Birimian granitoids within the southern West African Craton [3] [32] [33]. The coexistence of TTG-type granodiorite, diorite, and granitic facies suggests a polyphase magmatic system involving multiple sources and processes. According to the genetic classification of [34], the Zoukougbeu granitoids are primarily of crustal derivation, yet the occurrence of dioritic intrusions points to a mantle-derived mafic contribution [35] [36]. This interpretation agrees with the dual crustal-mantle origin proposed for granitoids from the Tiassalé region [37] [38], suggesting a consistent magmatic evolution across the southern Birimian domain. The rocks are enriched in large-ion lithophile elements (LILEs) and display negative anomalies in Nb and Ti, accompanied by LREE-enriched patterns—features diagnostic of magmatic arcs related to subduction zones [39] [40]. Such geochemical characteristics indicate derivation from a hydrous, oxidized magma, consistent with melting of a basaltic crust in a convergent setting. This magmatic evolution implies a geodynamic environment dominated by arc magmatism, where crustal reworking and magma mixing were likely key in generating the observed compositional diversity.

5.3. Tectonic and Petrogenetic Implications

The integration of petrographic and geochemical data provides compelling evidence that the Zoukougbeu granitoids crystallized in a subduction-related continental arc setting during the Eburnean orogeny. The Pearce [41] discrimination diagram unequivocally places the Zoukougbeu granitoids within the volcanic arc granite (VAG) field (**Figure 7(a)** and **Figure 7(b)**), further confirming their sub-

duction-related affinity. On the Martin discrimination diagram [42] (**Figure 8**), the granodiorites, diorites, and gneisses plot within the Archean TTG domain, whereas the granites fall within the transitional Archean-post-Archean field, indicating a TTG-like protolith derived from partial melting of hydrated basaltic crust in a subduction regime. These results corroborate the model proposed by [43] for the Daloa granitoids, in which TTG magmas originated through subduction-driven melting processes. The Zoukougbeu granitoids likely represent the differentiation products of such TTG magmas, subsequently modified by fractional crystallization and limited crustal assimilation. The coexistence of TTG-like granodiorites with mantle-derived diorites underscores the hybrid nature of the magma sources, reflecting the interplay between mantle input and crustal anatexis during Paleoproterozoic crustal growth. This hybridization process is a defining feature of Birimian magmatic arcs, marking the progressive stabilization of the southern West African Craton through the accretion of juvenile arc terranes. Consequently, the Zoukougbeu granitoids can be interpreted as part of a paleosubduction system, representing the deep-seated expression of arc-related magmatism and crustal differentiation during the Eburnean orogenic cycle (ca. 2.1 - 2.0 Ga). This event was pivotal in constructing the continental crust of the southern West African Craton and establishing the metallogenic framework favorable for subsequent gold mineralization. According to studies by [12], the Daloa area, located east of the Sassandra Fault, represents a transition zone between the Archean and Birimian terrains. [43] further interprets the Daloa zone as a suture between these two terrains, structured by the thermal activity associated with the emplacement of the Sassandra Fault. This thermal influence is evidenced by the presence of migmatites in the Zoukougbeu area. Consequently, the impact of the Sassandra Fault is clearly observable in the Zoukougou region through widespread metamorphism and the development of secondary or associated faults.

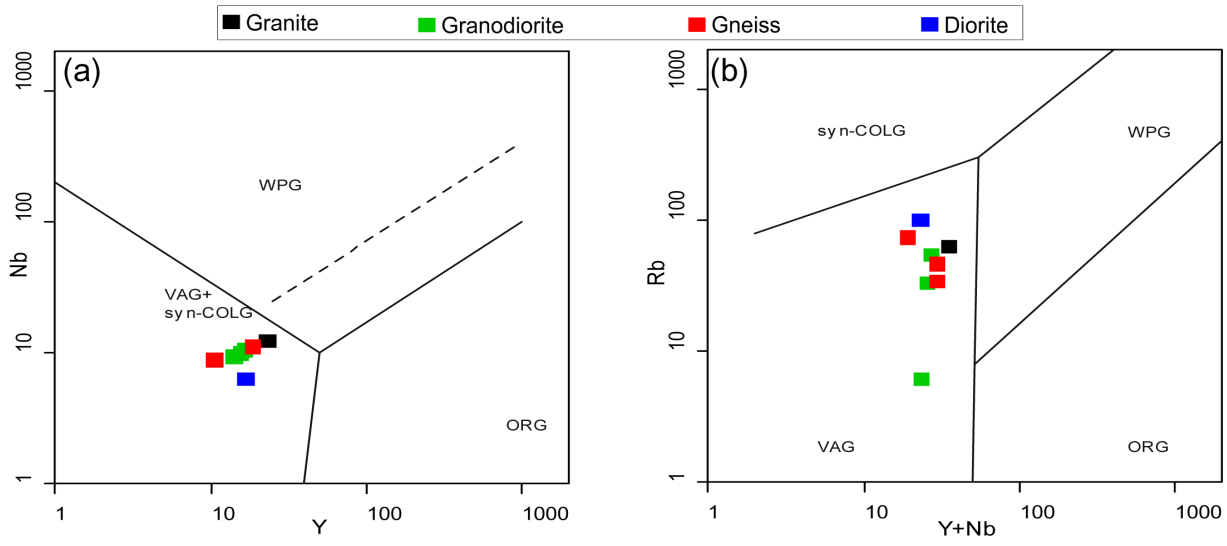

Figure 7. Tectonic discrimination diagrams for the Zoukougbeu studied rocks. (a) Nb vs. Y plot; (b) Rb vs. (Yb + Nb) plot (after [41]).

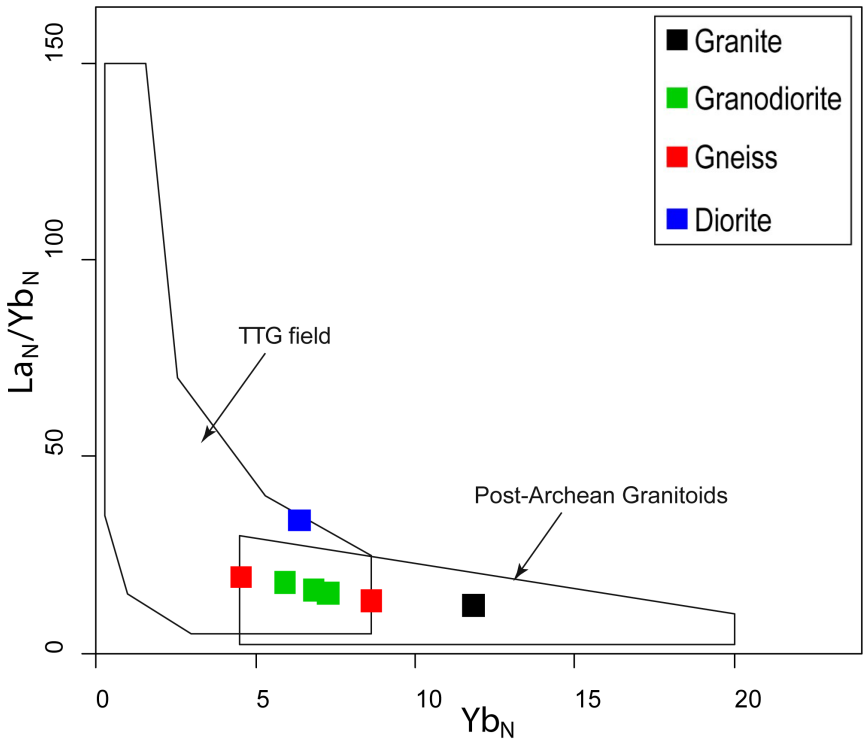

Figure 8. Position of the Zoukougbeu studied rocks on the (La/Yb)N vs. (Yb)N diagram (after [42]).

6. Conclusion

Petrographic and geochemical data from the Paleoproterozoic granitoids of the Zoukougbeu area provide new insights into their petrogenesis and tectonic significance. The studied rocks comprise a calc-alkaline, metaluminous to weakly peraluminous suite dominated by TTG-type granodiorites and gneisses, with subordinate granites, diorites, and pegmatites. Their mineralogical assemblages and alteration features reflect syn- to post-magmatic deformation and hydrothermal processes under greenschist to amphibolite facies conditions. Major and trace element systematics reveal coherent patterns—LILE enrichment and HFSE depletion—typical of subduction-related magmatism. The negative Eu anomalies and HREE depletion suggest plagioclase fractionation and a hydrous, oxidized magma source. These characteristics point to derivation from partial melting of a hydrated basaltic crust, with possible mantle interaction, in a continental volcanic-arc setting during the Eburnean orogeny. The coexistence of TTG-like and dioritic magmas underscores a hybrid crust-mantle contribution to magmatism, consistent with arc accretion and crustal reworking during Paleoproterozoic crustal growth. Thus, the Zoukougbeu granitoids record a critical episode of magmatic differentiation and continental stabilization in the southern West African Craton, contributing to the broader understanding of Eburnean geodynamics and associated metallogenic processes. To further refine this petrogenetic model, future research should prioritize high-precision geochronology (e.g., U-Pb on zircon) coupled

with detailed isotopic studies (Nd-Sr-Hf) to precisely constrain the timing of magmatism and quantitatively assess the contributions of their diverse source components.

Conflicts of Interest

The authors declare no conflicts of interest regarding the publication of this paper.

References

[1] Liégeois, J.-P., Benhallou, A., Azzouni-Sekkal, A., Yahiaoui, R. and Bonin, B. (2005) The Hoggar Swell and Volcanism: Reactivation of the Precambrian Tuareg Shield during Alpine Convergence and West African Cenozoic Volcanism. In: Foulger, G.R., *et al.*, Eds., *Plates, Plumes and Paradigms*, Geological Society of America, 379-400. https://doi.org/10.1130/0-8137-2388-4.379

[2] Bessoles, B. (1977) Geologie de l'afrique. Le craton ouest africain. Geologie de l'afrique. Le craton ouest africain.

[3] Gasquet, D., Barbey, P., Adou, M. and Paquette, J.L. (2003) Structure, Sr-Nd Isotope Geochemistry and Zircon U-Pb Geochronology of the Granitoids of the Dabakala Area (Côte D'ivoire): Evidence for a 2.3 Ga Crustal Growth Event in the Palaeoproterozoic of West Africa? *Precambrian Research*, **127**, 329-354. https://doi.org/10.1016/s0301-9268(03)00209-2

[4] Feybesse, J.-L., Milési, J.-P., Johan, V., Dommanget, A. and Calvez, J.-Y. (1989) La limite Archéen/Protérozoïque inférieur d'Afrique de l'Ouest: Une zone de chevauchement majeure antérieure à l'accident de Sassandra; l'exemple des régions d'Odiénné et de Touba (Côte-d'Ivoire). *Comptes rendus de l'Académie des sciences. Série* 2, *Mécanique, Physique, Chimie, Sciences de l'univers, Sciences de la Terre*, **309**, Article No. 18.

[5] Hirdes, W., Davis, D.W. and Eisenlohr, B.N. (1992) Reassessment of Proterozoic Granitoid Ages in Ghana on the Basis of U/Pb Zircon and Monazite Dating. *Precambrian Research*, **56**, 89-96. https://doi.org/10.1016/0301-9268(92)90085-3

[6] Brou, K.J., Kouamelan, A.N. and Teha, K.R. (2024) Geochemistry of Micas from Issia Granite Complexe: A Marker of Geodynamic Evolution. *Open Journal of Geology*, **14**, 787-804. https://doi.org/10.4236/ojg.2024.148034

[7] Doumbia, S., Pouclet, A., Kouamelan, A., Peucat, J.J., Vidal, M. and Delor, C. (1998) Petrogenesis of Juvenile-Type Birimian (Paleoproterozoic) Granitoids in Central Côte-D'ivoire, West Africa: Geochemistry and Geochronology. *Precambrian Research*, **87**, 33-63. https://doi.org/10.1016/s0301-9268(97)00201-5

[8] Dago, A.G.B. and Coulibaly, Y. (2019) Typologie pétrographique et géochimique des granitoïdes de la région de Daloa au Centre-Ouest de la Côte d'Ivoire. 14.

[9] Baratoux, L., Jessell, M.W. and Kouamelan, A.N. (2024) The West African Craton. In: Hamimi, Z., *et al.*, Eds., *Regional Geology Reviews*, Springer International Publishing, 47-68. https://doi.org/10.1007/978-3-031-48299-1_3

[10] Lemoine, S. (1988) Evolution geologique de la region de dabakala (ne de la cote d'ivoire) au proterozoique inferieur. Possibilites d'extension au reste de la cote d'ivoire et au burkina faso: Similitudes et differences; les lineaments Greenville ferkessedougou et grand Cess-Niakaramandougou.

[11] Yacé, I. (2002) Initiation à la géologie: L'exemple de la Côte d'Ivoire et de l'Afrique de l'Ouest. Ceda.

[12] Kouamelan, A.N., Delor, C. and Peucat, J. (1997) Geochronological Evidence for Reworking of Archean Terrains during the Early Proterozoic (2.1 Ga) in the Western Côte D'ivoire (Man Rise-West African Craton). *Precambrian Research*, **86**, 177-199. https://doi.org/10.1016/s0301-9268(97)00043-0

[13] Ennih, N. and Liégeois, J. (2001) The Moroccan Anti-Atlas: The West African Craton Passive Margin with Limited Pan-African Activity. Implications for the Northern Limit of the Craton. *Precambrian Research*, **112**, 289-302. https://doi.org/10.1016/s0301-9268(01)00195-4

[14] Milési, J.-P., Ledru, P., Feybesse, J., Dommanget, A. and Marcoux, E. (1992) Early Proterozoic Ore Deposits and Tectonics of the Birimian Orogenic Belt, West Africa. *Precambrian Research*, **58**, 305-344. https://doi.org/10.1016/0301-9268(92)90123-6

[15] Ahimon, O. (1990) Notice explicative de la carte géologique de la Côte d'Ivoire au 1/200000, feuille Daloa. Mém. Dir. Géol.

[16] Middlemost, E.A.K. (1994) Naming Materials in the Magma/Igneous Rock System. *Earth-Science Reviews*, **37**, 215-224. https://doi.org/10.1016/0012-8252(94)90029-9

[17] O'connor, J. (1965) A Classification for Quartz-Rich Igneous Rocks Based on Feldspar Ratios. US Geological Survey Professional Paper 525, 79-84. https://www.scirp.org/reference/referencespapers?referenceid=3246754

[18] Peccerillo, A. and Taylor, S.R. (1976) Geochemistry of Eocene Calc-Alkaline Volcanic Rocks from the Kastamonu Area, Northern Türkiye. *Contributions to Mineralogy and Petrology*, **58**, 63-81. https://doi.org/10.1007/bf00384745

[19] Maniar, P.D. and Piccoli, P.M. (1989) Tectonic Discrimination of Granitoids. *Geological Society of America Bulletin*, **101**, 635-643. https://doi.org/10.1130/0016-7606(1989)101<0635:tdog>2.3.co;2

[20] Alexis N'dri, K., Zhang, D., Zhang, T., Soh Tamehe, L., Serge Kouamelan, K., Wu, M., *et al.* (2021) Gold Mineralization in the Northern Margin of the North China Craton: Influence of Alkaline Magmatism and Regional Tectonic during Middle Paleozoic-Mesozoic. *Ore Geology Reviews*, **133**, Article ID: 103969. https://doi.org/10.1016/j.oregeorev.2020.103969

[21] Sun, S.-S. and McDonough, W.F. (1989) Chemical and Isotopic Systematics of Oceanic Basalts: Implications for Mantle Composition and Processes. *Geological Society, London, Special Publications*, **42**, 313-345. https://doi.org/10.1144/gsl.sp.1989.042.01.19

[22] Boynton, W.V. (1984) Cosmochemistry of the Rare Earth Elements: Meteorite Studies. In: *Developments in Geochemistry*, Elsevier, 63-114. https://doi.org/10.1016/b978-0-444-42148-7.50008-3

[23] Tapé, B. (2017) Caractérisation de la minéralisation aurifère du prospect Abujar, permis de Zoukougbeu (région de Daloa, Centre-Ouest de la Côte d'Ivoire). Master, Université Félix Houphouët-Boigny.

[24] Ehouinsou, K.F. (2018) Étude pétro-structurale et métallogénique du prospect aurifère d'Abujar, Permis de Zoukougbeu (Daloa, Centre-Ouest de la Côte d'Ivoire). Mémoire de Master, Université Félix Houphouët-Boigny, 65 p.

[25] Keita, A.K. (2020) Pétrographie, structurale, et cartographie du prospect aurifère d'Abujar, permis de Zoukougbeu (Daloa, centre-ouest de la Côte d'Ivoire). Master, Université Félix Houphouët-Boigny.

[26] Ouattara, Z. and Coulibaly, Y. (2018) Apport des minéraux d'altération dans la caractérisation du gisement d'or de Bonikro, sillon birimien de Fettèkro, Côte d'Ivoire.

[27] Sylla, M. and Ngom, P.M. (1997) Le gisement d'or de Sabodala (Sénégal Oriental):

Une minéralisation filonienne d'origine hydrothermale remobilisée par une tectonique cisaillante. *Journal of African Earth Sciences*, **25**, 183-192. https://doi.org/10.1016/s0899-5362(97)00097-3

[28] Hirst, T. (1942) The Geology of the Konongo Gold Belt and Surrounding Country. HM Stationery Office. 50 Hoffer, G., 2008. Fusion partielle d'un manteau métasomatisé par un 50 liquide adakitique: Approches géochimique et expérimentale de la genèse et de l'évolution des magmas de l'arrière-arc équatorien. Thèse de Doctorat, University Blaise Pascal.

[29] Leube, A., Hirdes, W., Mauer, R. and Kesse, G.O. (1990) The Early Proterozoic Birimian Supergroup of Ghana and Some Aspects of Its Associated Gold Mineralization. *Precambrian Research*, **46**, 139-165. https://doi.org/10.1016/0301-9268(90)90070-7

[30] Bourges, F., Debat, P., Tollon, F., Munoz, M. and Ingles, J. (1998) The Geology of the Taparko Gold Deposit, Birimian Greenstone Belt, Burkina Faso, West Africa. *Mineralium Deposita*, **33**, 591-605. https://doi.org/10.1007/s001260050175

[31] Baratoux, L., Metelka, V., Naba, S., Jessell, M.W., Grégoire, M. and Ganne, J. (2011) Juvenile Paleoproterozoic Crust Evolution during the Eburnean Orogeny (~2.2 - 2.0 Ga), Western Burkina Faso. *Precambrian Research*, **191**, 18-45. https://doi.org/10.1016/j.precamres.2011.08.010

[32] Sylvester, P.J. and Attoh, K. (1992) Lithostratigraphy and Composition of 2.1 Ga Greenstone Belts of the West African Craton and Their Bearing on Crustal Evolution and the Archean-Proterozoic Boundary. *The Journal of Geology*, **100**, 377-393. https://doi.org/10.1086/629593

[33] Kouadio, F.J.-L.H. (2017) Étude Pétrostructurale des formations géologiques du Sudouest de la Côte d'Ivoire (secteur Bliéron-Grand-Béréby): Apport de la géochimie et du couple Déformation-métamorphisme. These de Doctorat, Université Félix Houphouet Boigny.

[34] Barbarin, B. (1990) Granitoids: Main Petrogenetic Classifications in Relation to Origin and Tectonic Setting. *Geological Journal*, **25**, 227-238. https://doi.org/10.1002/gj.3350250306

[35] Bussy, F. (1990) Pétrogenèse des enclaves microgrenues associées aux granitoïdes calco-alcalins: Exemple des massifs varisques du Mont blanc (Alpes Occidentales) et mio-cène du Monte Capanne (Île d'Elbe, Italie). Thèse de Doctorat, Université de Lausanne.

[36] Abdallah, N. (2008) Géochimie et géochronologie des intrusions magmatiques panafricaines du terrane Egéré-Aleskod: Exemple des massifs granitiques de l'Onane, Tihoudaine et Tisselliline (Hoggar entral, Algérie). These de doctorat, Universte des sciences et de la technologie Houari Boumedienne.

[37] Ouattara, G. and Koffi, G.B. (2014) Typologie des granitoïdes de la région de Tiassalé (Sud de la Côte d'Ivoire—Afrique de l'Ouest): Structurologie et Relations Gé-nétiques. *Afrique Science*, **10**, 258-276.

[38] Raoul, T.K., Nicaise, K.A., Ephrem, A.M., Chérubin, D.S., Nestor, H.N., Augustin, K.Y., *et al.* (2018) Caractères pétrographiques et géochimiques des granitoïdes birimiens du bassin de la Comoé et environs (Sud de la Côte d'Ivoire). *International Journal of Engineering Science Invention*, **7**, 16-25.

[39] Hoffer, G. (2008) Fusion partielle d'un manteau métasomatisé par un liquide adakitique: Approches géochimique et expérimentale de la genèse et de l'évolution des magmas de l'arrière-arc équatorien. Thèse de Doctorat, Université Blaise Pascal-Clermont-Ferrand II.

[40] Dupuis, C. (2005) Pétrologie et géochimie des provinces mésozoïques téthysiennes reliées à la zone de suture Yarlung-Zangbo, Tibet. PhD, Université Laval.

[41] Pearce, J.A., Harris, N.B.W. and Tindle, A.G. (1984) Trace Element Discrimination Diagrams for the Tectonic Interpretation of Granitic Rocks. *Journal of Petrology*, **25**, 956-983. https://doi.org/10.1093/petrology/25.4.956

[42] Martin, H. (1987) Evolution in Composition of Granitic Rocks Controlled by Time-Dependent Changes in Petrogenetic Processes: Examples from the Archaean of Eastern Finland. *Precambrian Research*, **35**, 257-276. https://doi.org/10.1016/0301-9268(87)90058-1

[43] Dago, A.G.B. (2020) Les granitoïdes Birimiens de la région de Daloa (centre-ouest de la Côte d'Ivoire): Genèse et implication dans l'évolution thermique du Craton ouest Africain. Thèse unique, Université felix houphouët-Boigny de Cocody.

Appendix

Table S1. Geochemical data.

Sample	ZOU06	ZOU11	ZOU15	ZOU23	ZOU10	ZOU12	ZOU17	ZOU16
Litho	Granite		Granodiorite		Gneiss		Diorite	
SiO_2	75	63.61	63.16	64.74	64.73	67.23	63.79	52.72
Al_2O_3	12.77	15.1	14.29	14.33	14.05	14.79	14.74	12.96
Fe_2O_3	2.14	5.94	5.43	5.66	5.59	4.53	6.67	7.21
MnO	0.04	0.09	0.07	0.06	0.11	0.06	0.13	0.12
MgO	0.57	2.94	2.29	2.98	2.32	2.53	2.92	6.4
CaO	2.32	5.51	4.55	4.61	7.01	5.24	4.69	7.92
Na_2O	3.95	4.2	6.77	3.65	2.5	1.59	4.18	3.31
K_2O	1.91	0.89	0.34	1.64	1.51	2.54	0.98	2.45
TiO_2	0.14	0.65	0.57	0.62	0.58	0.5	0.68	0.7
P_2O_5	0.029	0.161	0.02	0.155	0.135	0.144	0.192	0.515
PF	0.86	0.64	1.8	1.39	1.46	0.74	0.75	4.89
Total	99.73	99.73	99.29	99.84	100	99.89	99.72	99.2
As	0.7	X	1.5	X	0.7	0.9	X	0.6
Ba	619.6	524.1	127.8	555	733.8	720.2	521.9	1138.7
Be	1.91	1.37	0.55	1.11	1.24	1.11	1.18	1.35
Bi	0.16	0.07	0.48	0.23	0.1	0.16	0.19	0.14
Cd	0.08	0.1	0.08	0.09	0.1	0.07	0.11	0.09
Ce	92.6	71.8	68.1	73.6	75.5	55.4	75.5	148.1
Co	3.4	20.1	17.9	19	17.1	12.1	23.3	30
Cr	33	56	51	98	117	31	88	350
Cs	8.7	2.9	0.3	2	1.4	2	1.5	6.7
Cu	12	37	10	6	28	21	25	37
Dy	3.9	3	2.6	2.9	3.3	2	3.4	4.2
Er	2.3	1.7	1.6	1.8	1.9	1	2.1	1.7
Eu	1	1.1	1.1	1.2	1.1	1	1.3	3
Ga	15.4	17	20.4	16.8	16.3	18.1	17.4	17.5
Gd	4.4	3.8	3.2	3.5	4	2.7	4.3	7.5
Ge	1.3	1.03	1.91	1.08	0.95	1.66	1.13	1.22
Hf	3.9	4.4	3.9	4.9	4.7	4.4	4.4	3.9
Ho	0.8	0.6	0.5	0.6	0.7	0.4	0.7	0.7
In	0.02	0.04	0.02	0.04	0.05	0.02	0.05	0.05
La	47.4	36.1	35	36.5	38	28.9	38.2	70.8
Lu	0.4	0.2	0.2	0.3	0.3	0.2	0.3	0.2

Continued

Mo	2	1	3.4	0.7	2	2.4	1	0.4
Nb	12.3	9.9	9.3	10.5	11.1	8.8	11.2	6.3
Nd	31	27.8	27.1	28.4	29.2	19.8	30	69.9
Ni	5.6	55.4	50.6	59.3	57.5	14.9	63.2	146.6
Pb	10	9.3	10.1	8.3	8.3	8.1	8.2	9.6
Pr	9.5	7.9	7.5	8	8.3	5.9	8.5	17.6
Rb	62.9	33.1	6.1	54.7	46	73.2	33.9	100.1
Sc	X	14	12	14	14	X	15	18
Sb	0.19	0.2	0.43	0.48	0.41	0.33	0.29	0.26
Sm	5.1	4.5	3.9	4.4	5.1	3.7	4.9	12.3
Sn	3	1	1	2	2	X	2	1
Sr	186.7	380.1	273.3	294.6	198.1	227.8	291.6	530.9
Ta	1.3	0.9	0.9	1	1	0.9	1.1	0.6
Tb	0.7	0.5	0.5	0.5	0.6	0.3	0.6	0.9
Th	11.4	6.3	6.5	7.3	7.2	4.9	7	13.3
Tm	0.3	0.3	0.2	0.3	0.3	0.2	0.3	0.2
U	3	1.7	1.6	1.9	1.6	1.5	2.3	3.3
V	14	103	48	97	101	66	107	152
W	2	1	62	6	1	3	2	4
Y	23	15.7	14.1	16.5	18.7	10.5	18.6	16.8
Yb	2.6	1.5	1.3	1.6	1.9	1	1.9	1.4
Zn	35	63	52	68	50	52	69	89
Zr	124	160	152	198	180	167	189	149
A/CNK	1	0.84	0.72	0.89	0.76	0.99	0.9	0.58
∑REE	202	160.8	152.8	163.6	170.2	122.5	172	338.5
Eu/Eu*	0.65	0.81	0.95	0.93	0.74	0.97	0.87	0.96
(La/Yb)N	12.29	16.23	18.15	15.38	13.48	19.48	13.55	34.09
(La/Sm)N	5.85	5.05	5.65	5.22	4.69	4.91	4.9	3.62
(Gd/Yb)N	1,365	2,043	1,987	1,763	1,698	2,179	1,826	4,322